Organic & Biomolecular Chemistry

Accepted Manuscript

This article can be cited before page numbers have been issued, to do this please use: S. Zhang, B. an, J. Li, J. Hu, L. huang, X. Li and A. S. C. Chan, *Org. Biomol. Chem.*, 2017, DOI: 10.1039/C7OB01655G.

ROYAL SOCIETY OF CHEMISTRY

rsc.li/obc

View Article Online
DOI: 10.1039/C7OB01655G

Journal Name

ARTICLE

Synthesis and Evaluation of Selenium-containing Indole Chalcone and Diarylketone Derivatives as Tubulin Polymerization Inhibition Agents

Received 00th January 20xx,
Accepted 00th January 20xx

DOI: 10.1039/x0xx00000x

www.rsc.org/

Shun zhang, Baijiao An, Jiayan Li, Jinhui Hu, Ling Huang,* Xingshu Li,* and Albert S. C. Chan

Sixteen new selenium-containing indole chalcone and diarylketone derivatives were synthesized and evaluated as tubulin polymerization inhibitor. Among them, compound **25b**, exhibited most potent antiproliferative activities against six human cancer cell lines with IC_{50} values of 0.004 - 0.022μM. Microtubule dynamics assay and immunofluorescence assay confirmed that **25b** could effectively inhibit tubulin polymerization (IC_{50} = 2.1± 0.27 μM). Further Cellular mechanism studies revealed that **25b** induced G2/M phase arrest, which was further evidenced by the decrease in the mitochondrial membrane potential (MMP).

Introduction

Cancer is a serious disease that is the second leading cause of human death after cardiovascular disorders. In past decades, many anticancer agents targeting different enzymes or receptors have been developed or are currently being developed. Among them, microtubule stabilizing or microtubule destabilizing agents have attracted much attention because microtubules play vital roles in the regulation of mitosis, disruption of microtubule dynamics, induction of cell cycle arrest in G2/M phase, formation of abnormal mitotic spindles, and signals for apoptosis.[1-2] Colchicine[3] is a typical tubulin inhibitor targeting the colchicine binding site, and Combretastatin A-4 (CA-4) (Fig. 1), which was first isolated from the bark of the African willow tree *Combretum caffrum* in 1989, exhibits potent tubulin polymerization inhibition and binds to the same binding site as colchicine.[4,5] To develop novel and more effective anticancer agents, many studies on the modification of CA-4 have appeared in recent years.[6-10]

Selenium (Se) is an essential trace mineral nutrient with multiple roles in the growth and function of living animal cells, e.g., providing protection from free radical-induced cell damage.[11-12] It is known that there are twenty-five selenoproteins in the human body with specific biological functions. Selenium compounds have been used as promising chemo-preventive agents for some diseases. Some animal experiments have indicated that organoselenium has a higher bio-disposability and biological activity than Se in inorganic compounds. In recent years, the potential cancer therapeutic effects of selenium is attracting more and more attention, and several organoselenium compounds have been shown to inhibit cancer cell growth in various xenograft rodent models for different cancer types. [13-17] Also, some reports showed that selenium has a protective effect in chemotherapy of some types of cancer.

Indole and its derivatives have a wide range of biological activities. Some naturally occurring indole alkaloids including vincristine, vinblastine, vinorelbine and vindesine have gained FDA approval as drugs for anti-tumor activity. Synthetic drugs such as indomethacin (NSAID), ondansetron (chemotherapy induced nausea and vomiting), fluvastatin (hypercholesterolemia), and zafirlukast (leukotriene receptor antagonist), have also reached the patient's bedside.[18] Recently, indole derivatives were also studied as tubulin inhibitor. Jang-Yang Chang et al reported 4- and 5-aroylindoles (Fig. 1, compound **A**) as antitubulin agents.[19] In our previous work, we disclosed the evaluation of a series of indole-chalcone derivatives (Fig. 1, compound **B**) exerting effective antitumor activity through microtubule destabilization.[20]

Inspired by the extensive pharmacological activities of indole analogues and biological activities of Selenium, herein, we report the synthesis of a series of selenium-containing indole chalcone derivatives (Fig 1) and diarylketone derivatives (Fig 1). Subsequently, their antitumor activities are evaluated in vitro, and their underlying cytotoxic mechanisms are also elucidated.

School of Pharmaceutical Sciences, Sun Yat-sen University, Guangzhou 510006, China;
*For L. Huang: Tel.: +086-20-3994-3051; Fax: +086-20-3994-3051; e-mail: huangl72@mail.sysu.edu.cn; For X. Sh. Li: Fax: +086-20-3994-3050; Tel.: +086-20-3994-3050; E-mail: lixsh@mail.sysu.edu.cn

Electronic Supplementary Information (ESI) available: [details of any supplementary information available should be included here]. See DOI: 10.1039/x0xx00000x

View Article Online
DOI: 10.1039/C7OB01655G
ARTICLE Journal Name

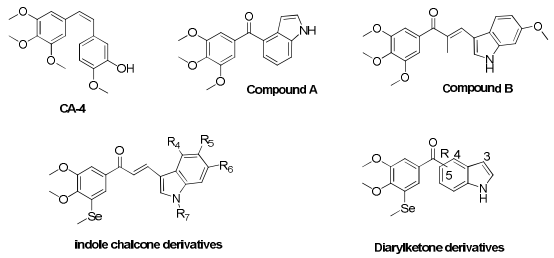

Fig 1 Structure of CA-4, representative compound of aroylindoles (A) and indole-chalcone derivatives (B), structural general formula of selenium-containing indole chalcone derivatives and diarylketone derivatives.

Results and discussion

Chemistry

The synthetic routes of the target compounds including twelve chalcone derivatives and four diarylketone derivatives are depicted in schemes 1-5. First, the selenium-containing key intermediate **6** was prepared from commercially available 4-hydroxy-3-methoxyacetophenone **1**. By the reaction of **1** with nitric acid in the presence of acetic acid, compound **2** was obtained in good yield, which was methylated by dimethylsulfate to afford **3**. The hydrogenation of 3 with iron in the presence of acetic acid gave amine intermediate **4**, which was diazotized and reacted immediately with KSeCN to provide ketone intermediate **5**. The reaction of **5** with CH_3I and $NaBH_4$ afforded **6** quickly and in good yield. Indole-3-carbaldehyde derivatives **8a-8c, 10a-10c** and **11a-11c** were prepared as shown in scheme 2. Commercially available compounds **7** reacted with methyl iodide and sodium hydride to give **8**. The reaction of commercially available substituted indole **9** with $POCl_3$ and DMF afforded **10**, which were treated with methyl iodide to provide the N-methyl products **11a-11c** (scheme 2)**.** Finally, the aldol condensation of selenium-containing intermediate **6** with indole-3-carbaldehyde derivatives **7**, **8**, **10** or **11** gave target compounds **12**, **13** and **14** (scheme 3).

The syntheses of diarylketone derivatives are summarized in schemes 4-5. First, selenium-containing bromobenzene derivatives **21** were prepared with the same procedures as the synthesis of **6** using 2-methoxy phenol as the starting material (scheme 4). Then, by treating with phenylsulfonyl chloride, indole-3-carbaldehyde analogues **7a-7c** were converted to their N-phenylsulfonyl derivatives **22a-22c**. Finally, target compounds **25a-25c** and **27** were obtained by treating intermediate **21** with **22a-22c** or **8b** in the presence of n-BuLi at -78°C, oxidizing the resulting alcohol by IBX and removing the protecting group from **23a-23c (**scheme 5).

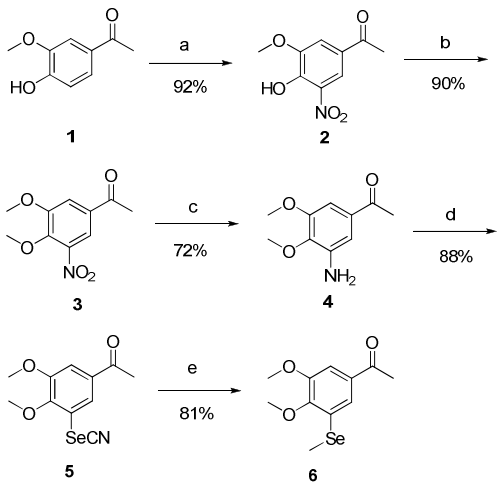

Scheme 1. The synthesis of intermediate compound **6**. Reagents and conditions: (a) HNO_3, AcOH, 3 h, r.t. (b) Dimethylsulfate, K_2CO_3, acetone, 2d, 80°C. (c) Fe, AcOH, 8 h, r.t. (d) i: HCl, H_2O, $NaNO_2$, 30 min, -5°C, ii: NaOAc, 30 min, 0°C, iii: KSeCN, 3 h, 0°C-r.t. (e) $NaBH_4$, CH_3I, EtOH, 2 min, r.t.

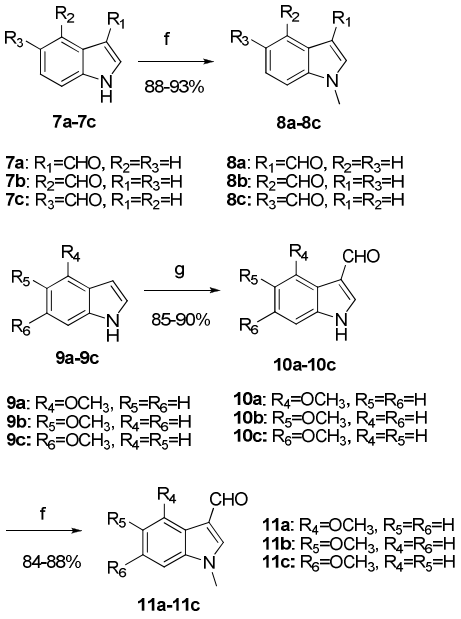

Scheme 2. The synthesis of intermediate compounds **8**, **10** and **11**. Reagents and conditions: (f) CH_3I, NaH, THF, 12 h, r.t. (g) $POCl_3$, DMF, 8 h, r.t.

View Article Online
DOI: 10.1039/C7OB01655G

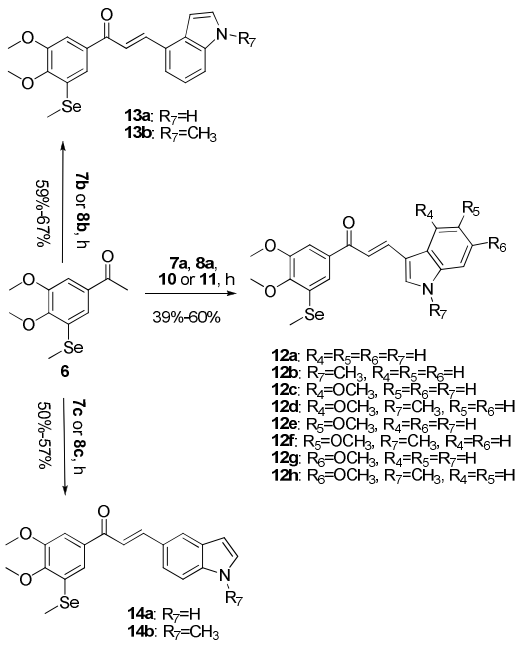

Scheme 3. The synthesis of target compounds **12**, **13** and **14**. Reagents and conditions: (h) Piperidine, AcOH, EtOH, 2-3d, 95°C.

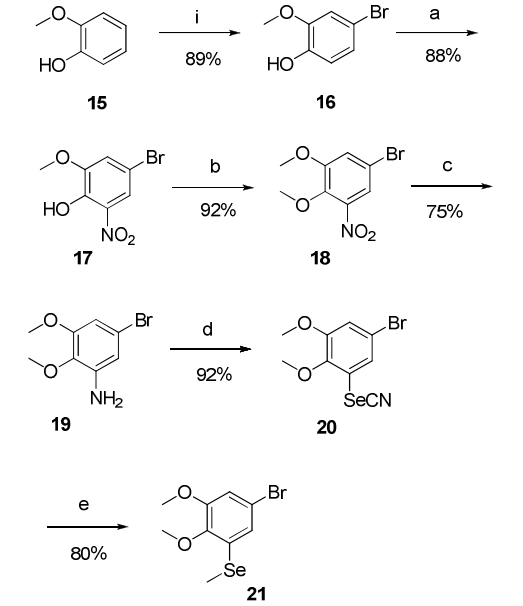

Scheme 4. The synthesis of intermediate compound **21**. Reagents and conditions: (i) NBS, CH_3CN, 2 h, 0°C, (a) HNO_3, AcOH, 3 h, r.t. (b) Dimethylsulfate, K_2CO_3, acetone, 2d, 80°C. (c) Fe, AcOH, 8 h, r.t. (d) i: HCl, H_2O, $NaNO_2$, 30 min, -5°C, ii: NaOAc, 30 min, 0°C, iii: KSeCN, 3 h, 0°C-r.t. (e) $NaBH_4$, CH_3I, EtOH, 2 min, r.t.

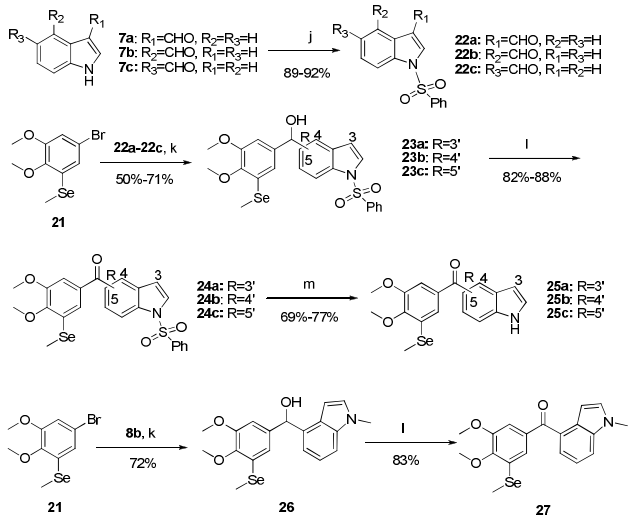

Scheme 5. The synthesis of target compounds **25a**-**25c** and **27**. Reagents and conditions: (j) phenylsulfonyl chloride, NaH, THF, 10 h, 0°C. (k) 1-(phenylsulfonyl)-1H-indole-4-carbaldehyde or 1-methyl-1H-indole-4-carbaldehyde, *n*-BuLi, dry THF, -78°C, 12 h. (l) IBX, THF, 2d. (m) NaOH, CH_3OH, 3 h, r.t.

Biological evaluation

In vitro growth inhibition of human cancer cell lines

The antiproliferative activities of the two series of compounds against six kinds of human cancer cell lines, including A549 (non-small-cell-lung cancer cell line), MDAMB-231 (human breast cancer cell line), HepG2 (human liver carcinoma cell line), HeLa (human epithelial cervical cancer cell line), HCT116 and RKO (human colon carcinoma cell line), were evaluated by MTT assay, and aroylindoles (Fig. 1, compound B) was used as the reference compounds. The results listed in Table 1 showed that most of the synthesized compounds exhibited excellent antiproliferative activity with IC_{50} values in the sub-micromol level. Among the twelve chalcone derivatives, compound **12a** exhibited the highest activity with the IC_{50} values ranging from 23 to 79 nM, which implied that the chalcone derivative from non-substituted indole-3-carbaldehyde is appropriate. Further investigation of the structure-activity relationships showed that the activity is related to the position of substituted groups on the indole rings. Compound **12b** exhibited slightly lower activities than **12a** indicating that N-methyl in the indole moiety is unfavorable. This similar phenomenon also appeared in other N-methyl and NH indole derivatives, for example, **12e** vs **12f** and **12g** vs **12h**. However, **12c** vs **12d** exhibited the opposite trend. It is interesting that compound **25b**, diarylketone derivatives derived from indole-4-carbaldehyde and (5-bromo-2,3-dimethoxyphenyl)(methyl)selane, provided the best results with IC_{50} values of 4 nM for A549 cell line, 6 nM for MM231, 13 nM for HEPG2, 22 nM for RKO, 21 nM for HCT116, and 7 nM for HELA, respectively. The antiproliferative activities of **25b** are much more potent than reference compound **A** (IC_{50} values of 25 nM for A549 cell line, 33 nM for MM231, 34 nM for HEPG2, 59 nM for RKO, 49 nM for HCT116,

View Article Online
DOI: 10.1039/C7OB01655G

and 28 nM for HELA, respectively) , which suggested that the introduction of selenium is beneficial to the antitumor activity. The better activities than its N-CH_3 analogue **27** also implied that the non-substituted indole-4-carbaldehyde may be the best choice for the preparation of this kind of tubulin polymerization inhibitors. Furthermore, compounds **25a** and **25c** gave relatively lower activities than **25b,** indicating that the joint position of benzoyl on the indole ring is important.

Prediction of the absorption of compound 25b

In order to estimating the drug-like properties of selenium-containing compound, we calculated Clog P, polar surface area (PSA), hydrogen-bond acceptor atoms (HBA) and hydrogen-bond donor atoms (HBD) of compound **25b**. The absorption level of **25b** was also predicted with the ADMET program in Discovery studio 2.1.[21] The results showed in table 2 that compound **25b** meet the requirements of Lipinski's rules and had a good absorption. The study of the PK profile in rats will be performed in plan.

Table 2 Physical properties and prediction of absorption of **25b**.

Calculation a	25b	Lipinski's rules
MW	374.3	≤ 450
Clog P	3.87	≤ 5.0
HBA	3	≤ 10
HBD	1	≤ 5
PSA	47.56	≤ 90
Absorption levelb	0	

[a] MW: molecular weight; clogP: calculated logarithm of the octanol-water partition coefficient; HBA: hydrogen-bond acceptor atoms; HBD: hydrogen-bond donor atoms; PSA: polar surface area; [b] Data are predicted by discovery studio 2.1 soft (Accelrys). 0: good absorption, 1: moderate absorption, 2 : low absorption, 3 : very low absorption.[21]

Effect of 25b on the inhibition of tubulin polymerization.

Numerous studies have demonstrated that the disruption of microtubule dynamics induces the activation of mitochondrial membrane potential complex and arrests the cell cycle in early mitosis. To confirm the targeting of the tubulin-microtubule system by the synthesized compounds, we chose **25b**, which exhibited the best antiproliferative activity in the MTT assay of the six human cancer cell lines. As illustrated in Fig. 2, when purified and unpolymerized tubulin was incubated at 37°C (control sample), the increased fluorescence intensity with time showed that tubulin polymerization had indeed occurred. When tubulin was incubated with **25b** at the specific concentrations, the increased tendency of the fluorescence intensity was obviously decreased with the increase of **25b**, with an IC_{50} value of 2.1± 0.27 μM, which exhibited similar activity with colchicine (IC_{50}: 3.01 ± 0.12 μM). These data indicated that **25b** could effectively inhibit tubulin polymerization and act as potential microtubule destabilizing agents.

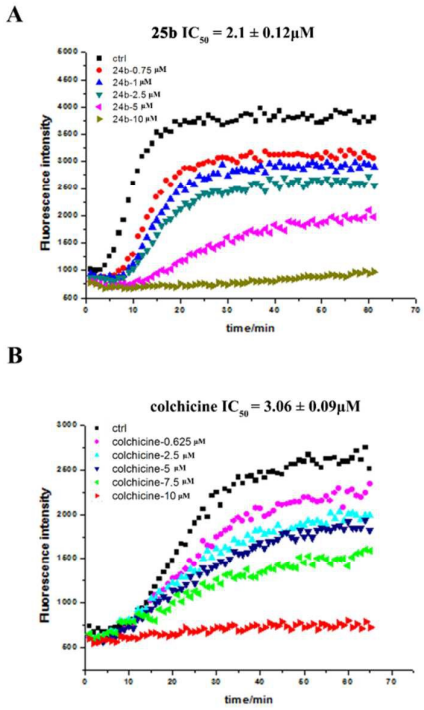

Fig. 2 In vitro tubulin polymerization assay. Tubulin in reaction buffer was incubated at 37°C in the absence (0.1% DMSO) or in the presence of 25b (10 μM, 5 μM, 2.5 μM, 1 μM, or 0.75 μM). The experiments were performed three times, and the results of representative experiments are shown.

Effect of 25b on Cell Cycle Progression

It is known that most tubulin destabilizing agents exhibit the ability to disrupt the regulated cell cycle distribution. As **25b** exhibited the most potent antiproliferative activities against six kinds of human cancer cell lines, we then investigated the effect of **25b** on cell cycle distribution by flow cytometry analysis. As shown in Fig. 3A, when HeLa cells were treated with 1 to 10 nM **25b** for 24 h, compared with the control (DMSO), the accumulation of cells in the G_2/M phase increased sharply from 8.21% to 50.38%, with a concomitant decrease in G1 and S phase cells. This trend was more obvious after the incubation time was extended to 48 h (Fig. 3B). After the 48 h

View Article Online
DOI: 10.1039/C7OB01655G

treatment, most of the cells were arrested at the G2/M phase at relatively high concentrations (49.4% and 61.88% of G2/M cell cycle arrest were found for 5 and 10 nM **25b** treatments, Fig. 3B). Therefore, these results implied that **25b** induced cell cycle arrest at the G2/M phase.

Effect of 25b on Cell Apoptosis Progression.

According to the cell cycle analysis results above, we hypothesized that **25b** treatment might induce the apoptosis of HeLa cells. To evaluate this ability of compound **25b**, flow cytometry with propidium iodide (PI) and fluorescent immunolabeling of the protein annexin-V (V-FITC) was performed. After treating with various indicated concentrations of **25b** for 48 or 72 h, the HeLa cells were harvested, stained with Annexin V-FITC and PI, and analyzed by flow cytometry. It can be seen from Fig. 4A when the HeLa cells were incubated with **25b** at concentrations of 1, 5, and 10 nM or DMSO (0.01%) for 48 h, the percentages of early and late apoptosis cells were 5.89%, 13.47%, and 23.19%, respectively. The early and late apoptosis cells increased to 18.13%, 37.99%, and 71.33%, respectively, when the incubation time was extended to 72 h (Fig. 4B), which indicated that **25b** induced cell apoptosis in a concentration- and time-dependent manner.

Mitochondrial dysfunction plays a vital role in the progression of apoptosis. We therefore investigated the possible involvement of mitochondrial dysfunction in **25b**-induced apoptosis of the cells by quantitative MMPs (mitochondrial transmembrane potential) assay with JC-1 staining. As expected (Fig. 4D), a rapid collapse of MMP was detected when the HeLa cells were exposed to 5-10 nM of **25b** for 48 h, as a consequence of the opening of the permeability transition pores that accumulate fluorescent dye from its red aggregated to green-monomeric forms.

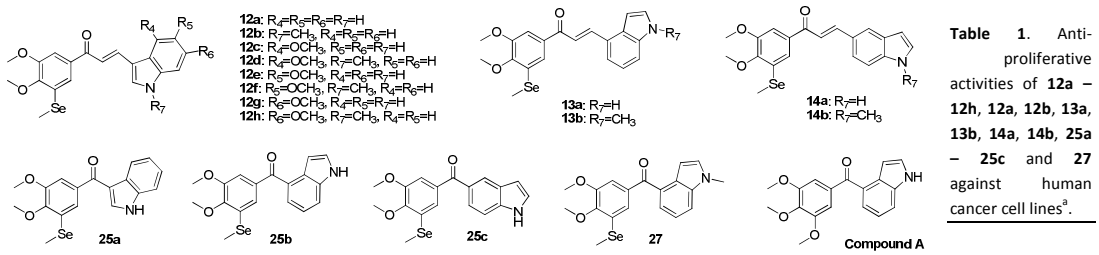

Table 1. Anti-proliferative activities of **12a – 12h**, **12a**, **12b**, **13a**, **13b**, **14a**, **14b**, **25a – 25c** and **27** against human cancer cell lines[a].

Entry	Comp.	Indole substitution position	A549	MDAMB-231	HepG2	RKO	HCT116	HeLa
1	**12a**	3	0.029 ± 0.002	0.038 ± 0.005	0.023 ± 0.003	0.032 ± 0.001	0.071 ± 0.002	0.059 ± 0.002
2	**12b**	3	0.041 ± 0.013	0.043 ± 0.002	0.085 ± 0.012	0.054 ± 0.015	0.087 ± 0.008	0.065 ± 0.007
3	**12c**	3	1.03 ± 0.034	1.41 ± 0.045	4.14 ± 0.162	2.61 ± 0.098	5.97 ± 0.035	4.30 ± 0.056
4	**12d**	3	0.344 ± 0.012	0.804 ± 0.023	2.39 ± 0.134	1.14 ± 0.0019	3.56 ± 0.043	1.86 ± 0.009
5	**12e**	3	1.44 ± 0.096	0.445 ± 0.068	0.314 ± 0.032	1.03 ± 0.098	1.78 ± 0.025	1.53 ± 0.078
6	**12f**	3	1.26 ± 0.034	0.912 ± 0.066	5.51 ± 0.177	1.28 ± 0.098	6.78 ± 0.14	3.49 ± 0.048
7	**12g**	3	0.098 ± 0.013	0.068 ± 0.007	0.115 ± 0.019	0.095 ± 0.004	0.095 ± 0.008	0.124 ± 0.005
8	**12h**	3	0.113 ± 0.007	0.077 ± 0.005	0.303 ± 0.015	0.093 ± 0.014	0.983 ± 0.006	0.288 ± 0.003
9	**13a**	4	0.191 ± 0.013	0.218 ± 0.12	1.14 ± 0.11	0.223 ± 0.018	1.85 ± 0.098	0.727 ± 0.07
10	**13b**	4	0.051 ± 0.034	0.046 ± 0.002	0.034 ± 0.014	0.044 ± 0.001	0.035 ± 0.019	0.037 ± 0.009
11	**14a**	5	0.083 ± 0.056	0.055 ± 0.023	0.044 ± 0.023	0.079 ± 0.014	0.054 ± 0.002	0.046 ± 0.002
12	**14b**	5	0.079 ± 0.014	0.048 ± 0.017	0.064 ± 0.018	0.094 ± 0.004	0.108 ± 0.017	0.086 ± 0.006
13	**25a**	3	0.027 ± 0.007	0.038 ± 0.002	0.056 ± 0.003	0.074 ± 0.003	0.089 ± 0.001	0.048 ± 0.009
14	**25b**	4	0.004 ± 0.001	0.006 ± 0.0012	0.013 ± 0.005	0.022 ± 0.007	0.021 ± 0.003	0.007 ± 0.002
15	**25c**	5	0.017 ± 0.007	0.016 ± 0.007	0.046 ± 0.007	0.052 ± 0.009	0.076 ± 0.015	0.063 ± 0.007
16	**27**	4	0.063 ± 0.004	0.087 ± 0.017	0.043 ± 0.006	0.093 ± 0.089	0.078 ± 0.004	0.050 ± 0.007
17	Comp. A	4	0.025 ± 0.003	0.033 ± 0.011	0.034 ± 0.006	0.059 ± 0.008	0.049 ± 0.009	0.028 ± 0.002

[a]Cell lines were treated with compounds for 48 h. Cell viability was measured by MTT assay as described in the Experimental Section. [b]IC_{50} values are indicated as the mean ± SD (standard error) of at least three independent experiments.

View Article Online
DOI: 10.1039/C7OB01655G

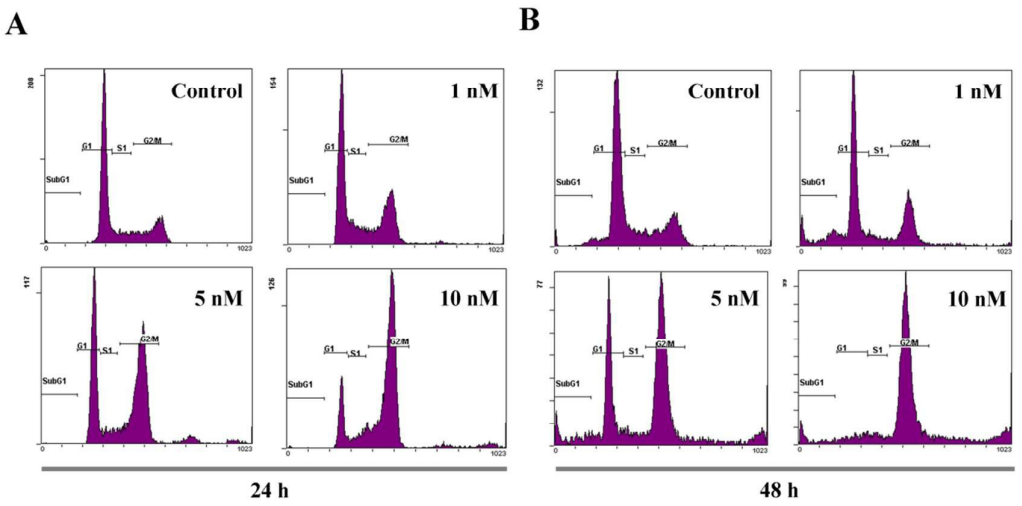

Fig. 3 Effect of **25b** on cell cycle progression. HeLa cells (3×10^5 cells/sample) were treated with specific concentrations of **25b** for 24 h (A) or 48 h (B). Cells were harvested, fixed with 70% ethanol, and stained with propidium iodide (PI). The cellular DNA content was then determined by flow cytometry.

View Article Online
DOI: 10.1039/C7OB01655G

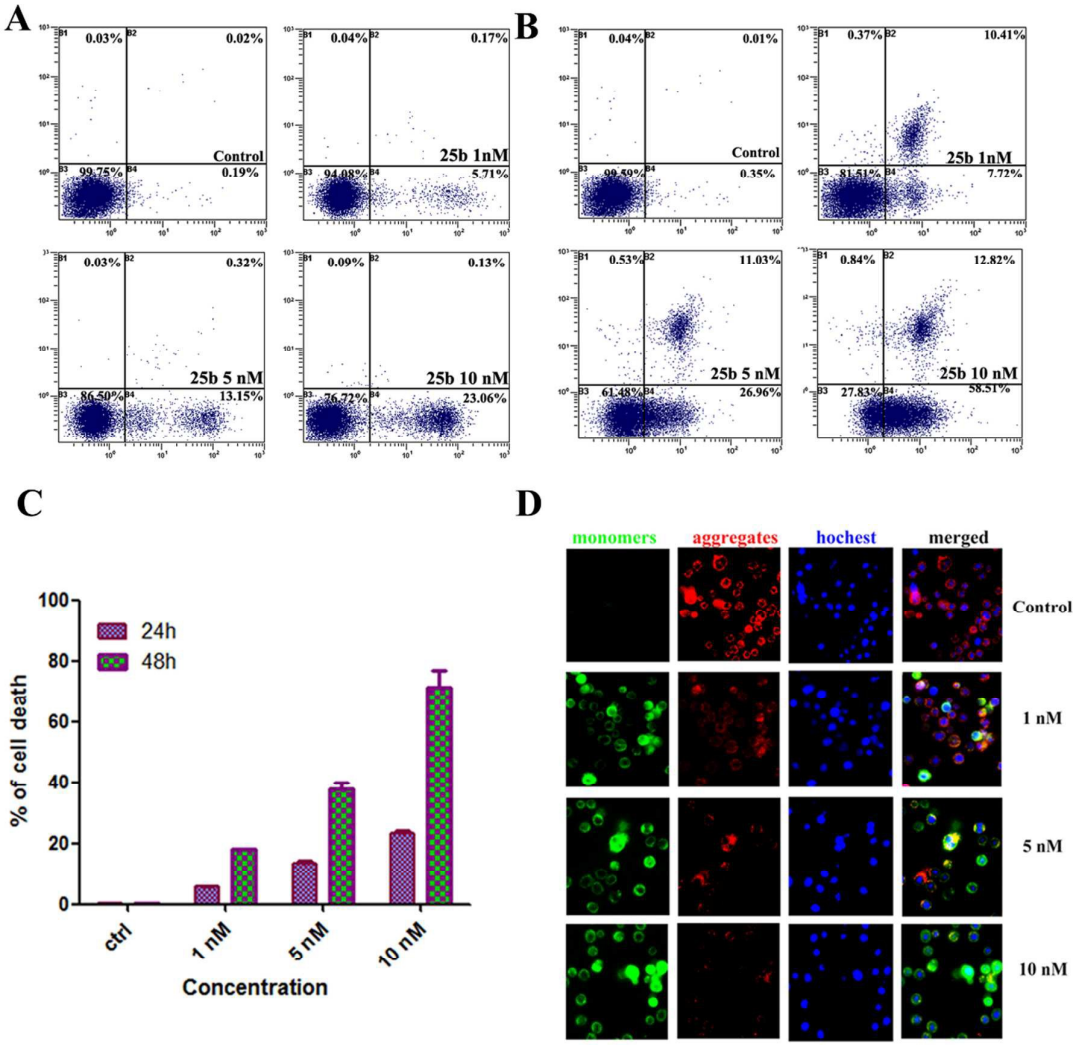

Fig. 4 Effect of **25b** on cell apoptosis progression and decreased mitochondrial membrane potential of HeLa cells. Induction of apoptosis in the cultured HeLa cells upon treatment with compound **25b**. Dot plot representation of Annexin-V-FITC-fluorescence (x-axis) vs PI-fluorescence (y-axis) of the apoptotic HeLa (Annexin-V positive) cells, treated with compound **25b** (1, 5 and 10 nM) for 24 h (A) or 48 h (B). The HeLa cells were treated with **25b** at different concentrations (1, 5, and 10 nM) or DMSO (0.01%) for 48 h, followed by incubation with the fluorescence probe JC-1 for 30 min. Then, the cells were analyzed by fluorescence microscopy (D). The experiments were performed at least three times, and the results of the representative experiments are shown

Effect of 25b on organization of cell microtubules

To study whether compound **25b** could disrupt the microtubule dynamics in living cells, we performed immunofluorescence assay in HeLa cells as the tubulin-microtubule system plays a vital role in the maintenance of cell shape and basic cellular functions. As shown in Fig. 5, the control group exhibited normal arrangement and organization of the microtubule network in the HeLa cells, which were characterized by regularly assembled, normal filiform microtubules wrapped around the uncondensed cell nucleus. In contrast, after exposure to **25b** for 24 h, the spindle formation demonstrated distinct abnormalities and was heavily disrupted. Especially, when the concentration increased to 10 nM, the microtubule spindles significantly shrunk around the center of the cells, and a number of dotted disorder formations were easily observed.

Conclusions

Considering that selenium is an essential trace mineral nutrient with multiple roles in the growth and function of living animal cells and it effectively inhibits tumorigenesis in both animal models and epidemiological studies, in this paper, we developed a series of selenium-containing chalcone and diarylketone derivatives on the basis of previous studies. The results of the antiproliferative activity assay in six human cancer cell lines showed that most of these synthesized compounds exhibited good to excellent activity. Among them, the optimal compound **25b** exhibited IC_{50} values of 0.004 to 0.022 μM for six cancer cell lines. Immunofluorescence assay showed that **25b** could effectively change the cell microtubules organization in HeLa cells. The cell cycle

View Article Online
DOI: 10.1039/C7OB01655G

progression in HeLa cells indicated that **25b** induced G2/M phase arrest, and cell apoptosis progression analysis showed that this was associated with a collapse of mitochondrial membrane potential (MMP). All of the above indicate that **25b** should be further studied for its drug abilities.

Comparing to the reference compound A, a remarkable effect of the oxygen by selenium substitution in **25b** was exhibited. Literatures have reported several mechanisms for the cancer therapeutic effects of selenium derivatives including oxidative stress, reduction of DNA damage, enhancement of the immune response, inflammation, incorporation into selenoproteins and so on. **25b** showed a typical tubulin polymerization inhibition responsible for the antiproliferative activity and its other mechanisms of that are under further study.

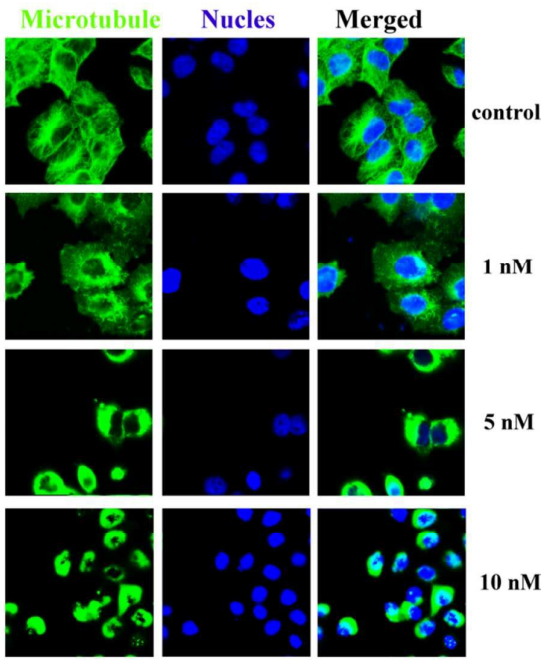

Fig. 5 Effects of **25b** on spindle microtubules and chromosome organization of HeLa cells. Cultured HeLa cells were incubated in the presence of varying concentrations of **25b** (1, 5, 10 nM) for 12 h. The spindle microtubules were stained for immunofluorescence using Alexa-Fluor 488 antibody (green) and corresponding Hoechst 33342 conjugate (blue), and the chromosomes were stained with DAPI (blue). Images were taken using an LSM 570 laser confocal microscope. The experiments were performed three times, and the results of representative experiments are shown.

Acknowledgements

We thank the National Natural Science Foundation of China (No. 21302235), Guangdong Natural Science Foundation (2014A030313124), Guangdong High-level personnel of special support program -Young top-notch talent project (2015TQ01R244), Guangzhou Pearl River New Star Fund Science And Technology Planning Project (201610010111) and The Fundamental Research Funds for the Central Universities (15ykpy04) for financial support of this study.

Notes and references

1 L. G. Wang, X. M. Liu, W. Kreis, D. R. Budman, *Cancer Chemoth. Pharm.*, 1999, **44**, 355–36**.**
2 S, Honore, E. Pasquier, D. Braguer, *Cell. Mol. Life Sci.*, 2005, **62**, 3039–3056.
3 T. Graening, H. G. Schmalz, *Angew. Chem. Int. Ed.*, 2004, **43**, 3230–3256.
4 G. R. Pettit, S. B. Singh, E. Hamel, C. M. Lin, D. S. Alberts, D. Garcia-Kendall, *Experientia,* 1989, **45**, 209-211.
5 G. R. Pettit, S. B. Singh, M. R. Boyd, E. Hamel, R. K. Pettit, J. M. Schmidt, F. Hogan, *J. Med. Chem.*, 1995, **38**, 1666-1672.
6 A. Brancale, R. Silvestri, *Med. Res. Rev.,* 2007, **27**, 209-238.
7 R. Kaur, G. Kaur, R. K. Gill, *Eur. J. Med. Chem.*, 2014, **87**, 89-124.
8 H. Chen, Y. Li, C. Sheng, *J. Med. Chem.*, 2013, **56**, 685-699.
9 B. L. Flynn, G. S. Gill, D. W. Grobelny, *J. Med. Chem.*, 2011, **54**, 6014-6027.
10 Y. S. Shan, J. Zhang, Z. Liu, *Curr. Med. Chem.*, 2011, **18**, 523-538.
11 G. V. Kryukov, S. Castellano, S. V. Novoselov, A. V. Lobanov, O. Zehtab, R. Guigó, V. N. Gladyshev, *Science*, 2003, **300**, 1439–1443.
12 C. Allmang, L. Wurth, *Biochim. Biophys. Acta*, 2009, **1790**, 1415–1423.
13 13. I. L. Clement, J. Donald Ganther, E. Howard, *Anticancer Res.*, 1998, **18**, 4019-4025.
14 N. Nguyen, A. Sharma, N. Nguyen, A. K. Sharma, D. Desai, S. J. Huh, S. Amin, C. Meyers, G. P. Robertson, *Cancer Prev. Res.*, 2011, **4**, 248-58.
15 T. Lin, Z. Ding, N. Li, J. Xu, G. Luo, J. Liu, J. Shen, *Eur. J. Cancer*, 2011, **47**, 1890-907.
16 C. Y. Chung, S. V. Madhunapantula, D. Desai, S. Amin, G. P. Robertson, *Cancer Prev. Res.*, 2011, **4**, 935-48;
17 H. Zeng, W. H. Cheng, L. K. Johnson, *J. Nutr. Biochem.*, 2013, **24**, 776-80.
18 18. N. Chadha, O. Silakari, *Eur. J. Med. Chem.*, 2017, **134**, 159-184.
19 J. P. Liou, C. Y. Wu, H. P. Hsieh, C. Y. Chang, C. M. Chen, C. C. Kuo, J. Y. Chang, *J. Med. Chem.*, 2007; **50**, 4548-4552.
20 J. Yan, J. Chen, S. Zhang, J. Hu, L. Huang, X. Li, *J. Med. Chem.*, 2016, **59**, 5264−5283.
21 42. W. J. Egan, K. M. Merz and J. J. Baldwin, *J. Med. Chem.*, 2000, **43**, 3867-3877.